www.ijprems.com
editor@ijprems.com

INTERNATIONAL JOURNAL OF PROGRESSIVE RESEARCH IN ENGINEERING MANAGEMENT AND SCIENCE (IJPREMS)
(Int Peer Reviewed Journal)
Vol. 05, Issue 10, October 2025, pp : 569-579

e-ISSN : 2583-1062
Impact Factor : 7.001

THE EFFECTS OF SORET AND HEAT SOURCE ON UNSTEADY MHD FLOW PAST A VERTICAL OSCILLATING PLATE IN POROUS MEDIUM

Sufiyanu Muhammad Dakin-Gari[1], Umar Sahabi[2], Abdullahi Ahmed[3], Usman Muhammad Layya[4]

[1,2,3,4]Department of Mathematics, Kebbi State Polytechnic, Dakingari, P.M.B. 1158, Kebbi State, Nigeria.

*Corresponding author email: Sufiyanumuhammad77@gmail.com

DOI: https://www.doi.org/10.58257/IJPREMS44228

ABSTRACT

A numerical analysis of unsteady magnetohydrodynamic (MHD) flow over a vertically oscillating plate within a porous medium is presented, incorporating the effects of heat sources and the Soret phenomenon. The coupled, nonlinear dimensionless governing equations were solved using an implicit finite difference method. Graphical representations of the velocity, temperature, and concentration profiles derived from the numerical solutions are provided and discussed. The impact of various physical parameters such as the magnetic field parameter, radiation parameter, Schmidt number, Prandtl number, Grashof number, heat source parameter, and Soret number is illustrated through graphs. It was observed during the computations that increasing the heat source parameter enhances both the fluid velocity and temperature, whereas increasing the magnetic field parameter results in a decrease in these quantities. Additionally, higher Soret number values lead to increases in both fluid velocity and concentration.

Keywords: Unsteady Flow, Porous Medium, MHD, Heat Source, Implicit Finite Difference.

1. INTRODUCTION

The investigation of magnetohydrodynamics (MHD) alongside mass and heat transfer, including the effects of radiation and diffusion, has attracted significant interest from researchers due to its broad range of applications. In astrophysics and geophysics, it is utilized to study stellar and solar phenomena, as well as radio wave propagation through the ionosphere. In engineering, MHD is applied in devices such as MHD pumps and bearings. The influence of radiation on MHD flow and heat transfer has gained increasing importance in industrial processes, particularly at high temperatures where radiation effects become prominent. Many engineering systems operate under such conditions, making it essential to understand radiation heat transfer for the development of efficient equipment. Examples include nuclear power plants, gas turbines, and various propulsion systems used in aircraft, missiles, satellites, and space vehicles (Sahin & Karabi, 2014).

When considering combined mass and heat transfer, fluid flow is primarily driven by density differences caused by gradients in concentration, temperature, or material composition. Mass diffusion is affected by changes in the thermal behavior of fluid particles, a phenomenon known as the Soret effect. As explained by Okuyade et al. (2018), the Soret effect plays a crucial role in engineering processes involving the simultaneous diffusion of mass and heat. It becomes particularly significant when certain species are present at the fluid's surface with densities lower than that of the surrounding fluid, thereby impacting overall transfer mechanisms and system dynamics.

2. REVIEW OF RELATED LITERATURE

The investigation of free convection flows in conjunction with oscillatory motion within porous media, especially in the presence of heat sources, has attracted increasing scholarly interest due to its wide-ranging practical applications in fields such as geophysics, solid mechanics, groundwater hydrology, oil recovery, thermal insulation, heat storage, and engineering (Chitra and Suhasini, 2018). Given the numerous applications of magnetohydrodynamic (MHD) oscillatory heat transfer flows, Usman and Sanusi (2023) recently explored how non-Newtonian nanofluid flows over a semi-infinite flat plate embedded in a porous medium affect heat radiation, Soret effects, and pressure forces. Bafakeeh et al. (2022) analyzed unsteady, hydromagnetic, oscillatory natural convection involving heat and mass transfer of a viscous electrically conducting fluid flowing along a vertical permeable plate, incorporating chemical reactions, thermal radiation, Hall currents, and Soret effects. Alwawi et al. (2020) investigated the natural convection of sodium alginate Casson nanofluids within a solid sphere under MHD conditions. Sharma et al. (2022) conducted an analytical study on time-dependent oscillatory free convection of viscous, incompressible, dissipative fluids passing through a porous medium-filled channel, accounting for heat generation and thermal radiation effects.

Research indicates that oscillatory flows can significantly enhance both mass and heat transfer rates. Such oscillations may be generated either by vibrating a solid object within a fluid or by inducing vibrations in the fluid around a stationary object, although the latter generally requires more energy. Extensive studies have demonstrated the

www.ijprems.com
editor@ijprems.com

INTERNATIONAL JOURNAL OF PROGRESSIVE RESEARCH IN ENGINEERING MANAGEMENT AND SCIENCE (IJPREMS)
(Int Peer Reviewed Journal)
Vol. 05, Issue 10, October 2025, pp : 569-579

e-ISSN : 2583-1062
Impact Factor : 7.001

importance of oscillating flows in various applications, including aerospace, military technology, high-performance heat exchangers, piston engines, chemical reactors, pulsating burners, Stirling engines, and cryogenic refrigeration systems. Khalid et al. (2017) examined free convection of micropolar fluids over an oscillating vertical plate, while Pradhan et al. (2017) studied unsteady free convection of a viscous, incompressible polar fluid flowing past a semi-infinite, moving, vertical porous plate. Krishna et al. (2019) investigated heat and mass transfer in MHD flow over a non-conducting, perpendicular flat porous surface. Noor et al. (2020) analyzed self-sustained convective flows driven by temperature gradients. Alwawi et al. (2020) again explored MHD natural convection involving sodium alginate Casson nanofluids within a solid sphere. Further, Fu and Tong (2017) numerically assessed how a transversely oscillating cylinder influences heat transfer from heated blocks within a planar duct. Bila et al. (2023) focused on improving heat transfer through MHD natural convection in a star-shaped enclosure with a heated baffle and MWCNT–water nanofluid. Pourgholam et al. (2015) performed numerical simulations on the effect of a rotating and oscillating blade on heat transfer from channel walls. Lastly, Jahangiri and Delbari (2020) conducted numerical analyses of flow and heat transfer in a mixing tank equipped with a helical single-blade mixer.

The distribution of thermal energy within a flowing fluid is influenced by the rate of heat generation at boundaries. This phenomenon is relevant in various manufacturing processes, including electronic chip fabrication and fire modeling. Heat waves propagate based on flow velocity and surface temperature, necessitating significant temperature differences for thermal radiation to occur. Consequently, heat generation and absorption often depend on the system's temperature and environmental conditions rather than remaining constant. Studies such as those by Nemati et al. (2021) have examined the effects of periodic magnetic fields combined with heat generation and absorption in non-Newtonian fluids. Elsayed et al. (2022) investigated how heat generation and absorption influence the boundary layer flow of nanofluids around a stretching cylinder. Khan et al. (2022) analyzed the impact of variable heat sources on the unsteady stagnation-point flow of magnetized Oldroyd-B fluids. Yasir et al. (2022) studied the effects of ohmic heating on double-diffusive nanofluid flow over a stretching cylinder. Additionally, Sheikholeslami (2022) found that increased heat absorption improves the thermal performance of solar thermal systems.

Another active research area involves enhancing convective heat transfer by moving a solid mass that acts as a heat source. Rahman and Tafti (2020) used numerical methods to explore heat transfer enhancement in a system with an oscillating, infinitesimally thin plate fin exposed to approaching flow. Amar et al. (2022) examined MHD heat transfer over a moving wedge with convective boundary conditions, considering viscous dissipation and internal heat generation or absorption. Sarhan et al. (2019) experimentally studied how vibrations of a rectangular flat plate affect convective heat transfer from the plate in horizontal and inclined positions. Hussain et al. (2022) analyzed the effectiveness of nonuniform heat generation and the thermal behavior of Carreau fluids flowing around a nonlinear elongating cylinder. Akcay et al. (2020) performed experiments on convective heat transfer from an oscillating vertical plate. More recently, Dakin-Gari et al. (2024) investigated the effect of heat sources on unsteady MHD free convection flow past a vertical oscillating plate through a porous medium using finite difference methods. This study aims to analyze unsteady MHD free convection flow past a vertically oscillating plate within a porous medium, incorporating the effects of a heat source and Soret phenomena. The governing equations for momentum, energy, and mass diffusion are solved using an implicit finite difference approach. The findings are presented through graphical representations, illustrating how various physical parameters influence the velocity, temperature, and concentration profiles of the fluid near the plates.

Statement of the Problem

The phenomena related to heat transfer flows are of paramount importance due to their wide-ranging applications in science and technology. These include critical industries such as food preservation, geothermal energy extraction, polymers manufacturing, and the cooling of nuclear reactors. Understanding and controlling heat transfer processes in these fields is essential for optimizing performance, ensuring safety, and advancing technological innovations. This study investigates the unsteady magneto-hydrodynamic (MHD) free convective flow of an incompressible, viscous fluid past a vertical oscillating plate embedded within a porous medium. The plate undergoes time-dependent oscillations which induce unsteady motion in the surrounding fluid. The porous medium's permeability influences the flow dynamics, adding complexity to the problem. Additionally, the presence of a magnetic field introduces Lorentz forces that oppose the flow, while heat sources within the medium contribute to thermal energy generation affecting temperature distributions. The analysis also considers the Soret effect (thermal diffusion) which causes mass flux due to temperature gradients, thereby impacting concentration profiles.

The primary objectives are to formulate the governing equations incorporating all relevant physical phenomena namely, unsteady flow, magnetic field effects, porous medium resistance, heat source, and Soret effect and to analyze how these factors influence the velocity, temperature, and concentration fields over time. The present study is the

www.ijprems.com
editor@ijprems.com

INTERNATIONAL JOURNAL OF PROGRESSIVE RESEARCH IN ENGINEERING MANAGEMENT AND SCIENCE (IJPREMS)
(Int Peer Reviewed Journal)
Vol. 05, Issue 10, October 2025, pp : 569-579

e-ISSN : 2583-1062
Impact Factor : 7.001

generalization of the mathematical model used by Muhammad et al., (2024) to incorporate the influence of Soret effect, on unsteady MHD flow past a vertical oscillating plate through a porous medium. The problem aims to deepen the understanding of heat and mass transfer characteristics in such complex systems, which are pertinent to various engineering and industrial applications involving MHD flows in porous structures with heat generation and diffusion effects.To the best of the authors' knowledge, this research has not been documented in any prior literature, thereby establishing its originality and contribution to the field.

3. METHODOLOGY

Mathematical Formulations

The current work examined the unstable one-dimensional flow via a porous media and a heat source of a viscous, incompressible, electrically conducting, radiating fluid past a vertical oscillating plate. The x and y axes in the Cartesian coordinate system should be taken normal to the plate and vertically upward along the plate, respectively. The irregular movement of a viscous incompressible fluid, initially at rest, around an infinite vertical plate with a concentration of C'_∞' and a temperature of T_∞.in a fixed state for the entire point. Additionally, it is assumed that the fluid's concentration and temperature are the same on the plate. When time $t' > 0$, the plate begins to oscillate at frequency ω' inside its own plane, and its temperature rises to T_w and the concentration level near the plate is raised linearly with respect to time. A transverse magnetic field of uniform strength B_o is assumed to be applied normal to the plate. The viscous dissipation and induced magnetic field are assumed to be negligible. The fluid is considered to be gray, absorbing/emitting radiation but a non-scattering medium. Under these assumptions, the equations governing the unsteady flow can be obtained as follows:

Momentum equation

$$\frac{\partial u'}{\partial t'} = v\frac{\partial^2 u'}{\partial y'^2} - \left(\frac{v}{k'} + \frac{\sigma B_o^2}{\rho}\right)u' + g\beta(T - T_\infty) + g\beta'(C' - C'_\infty) \quad (1)$$

Energy equation

$$\frac{\partial T'}{\partial t'} = \frac{K}{\rho c_p}\frac{\partial^2 T'}{\partial y'^2} - \frac{1}{\rho c_p}\frac{\partial q_r}{\partial y'} + \frac{Q'}{\rho c_p}(T - T_\infty) \quad (2)$$

Diffusion equation

$$\frac{\partial C'}{\partial t'} = D\frac{\partial^2 C'}{\partial y'^2} - K_1(C' - C'_\infty) + \frac{D}{v}\frac{\partial^2 T'}{\partial y'^2} \quad (3)$$

The corresponding initial and boundary conditions for the model are as follows:

$$\left\{\begin{array}{c} t' \le 0: u' = 0, T' = T'_\infty, C' = C'_\infty, \text{for all } y', \\ t > 0: \left\{\begin{array}{c} u' = u_o \cos\omega' t', T = T_w, \quad C' = C'_\infty + (C'_w - C'_\infty)At', \text{at } y' = 0 \\ u_o = 0, \ T \to T_\infty, \ C' \to C'_\infty, \quad \text{as } y' \to \infty \end{array}\right. \end{array}\right\} \quad (4)$$

Where, respectively, $x'$and y' represent the dimensional distances parallel and perpendicular to the plate. T' is the thermal temperature inside the thermal boundary layer and C' is the corresponding concentration; σ is the electric conductivity; C_p is the specific heat at constant pressure; D is the diffusion coefficient; $q_r$is the heat flux; Q' is the dimensional heat absorption coefficient; and K is the chemical reaction parameter. The velocity components in the $x'$and y' directions are u' and v', respectively; g is the gravitational acceleration; ρ is the fluid density; β and β' are the thermal and concentration expansion coefficients; and K' is the Darcy permeability.

The local radiant q_r for the case of an optically thin gray gas is expressed by Muthucumuraswamy and Geetha (2013).

$$\frac{\partial q_r}{\partial y'} = -4a^*\sigma\left(T'^4_\infty - T'^4\right) \quad (5)$$

It is assumed that, the temperature differences within the flow are sufficiently small such that T'^4 may be expressed as a linear function of the temperature T'_∞.This is obtained by expanding T'^4 in a Taylor series about T'_∞ and neglecting higher-order terms, thus:

$$T'^4 \cong 4T'^3_\infty T - 3T'^4_\infty. \quad (6)$$

Method of Solution

We incorporate the following non-dimensional variables and parameters in order to solve the governing equations in dimensionless form:

www.ijprems.com
editor@ijprems.com

INTERNATIONAL JOURNAL OF PROGRESSIVE RESEARCH IN ENGINEERING MANAGEMENT AND SCIENCE (IJPREMS)
(Int Peer Reviewed Journal)
Vol. 05, Issue 10, October 2025, pp : 569-579

e-ISSN : 2583-1062
Impact Factor : 7.001

$$\left\{\begin{array}{c} y=\frac{y'u_o}{v}, t=\frac{t'u_0^2}{v}, u=\frac{u'}{u_o}, \theta=\frac{T'-T'_\infty}{T'_w-T'_\infty}, Gc=\frac{g\beta^*(C'-C'_\infty)}{u_0^3}, \\ Gr=\frac{g\beta v(T-T_\infty)}{u_0^3}, C=\frac{(C'-C'_\infty)}{C'_w-C'_\infty}, Pr=\frac{\mu C_p}{k}, \quad Sc=\frac{v}{D}, K=\frac{u_0^2 K_1}{v^2} \\ R=\frac{16a^*v^2\sigma T'^3_\infty}{u_0^2}, K_r=\frac{v K_1}{u_0^2}, M=\frac{\sigma B_o^2 v}{\rho u_0^2} \quad Sr=\frac{D_m k_T}{vT_m}\left(\frac{T'_w-T'_\infty}{C'_w-C'_\infty}\right), \\ Q=\frac{Q'v^2}{U_0^2 k} \end{array}\right\} \quad (7)$$

The governing equations on using (9) into (1), (3), and using (5) - (8) into (2) reduce to

$$\frac{\partial u}{\partial t}=\frac{\partial^2 u}{\partial y^2}+Gr\theta+GmC-\left(\frac{1}{K}+M\right)u \quad (8)$$

$$\frac{\partial \theta}{\partial t}=\frac{1}{Pr}\frac{\partial^2\theta}{\partial y^2}+\frac{1}{Pr}(R+Q)\theta \quad (9)$$

$$\frac{\partial C}{\partial t}=\frac{1}{Sc}\frac{\partial^2 C}{\partial y^2}+Sr\frac{\partial^2\theta}{\partial y^2}-KrC \quad (10)$$

While the dimensionless initial and boundary conditions

$$\text{are}\left\{\begin{array}{l} t\le 0: u=0, \theta=0, C=0 \quad at\ y\le 0 \\ t>0:\left\{\begin{array}{l} u=0, \theta=1, \quad C=1 \quad at\ y=0 \\ u=0, \quad \theta=0, \quad C=0, \quad at\ y=1 \end{array}\right. \end{array}\right\} \quad (11)$$

Where Pr is the Prandtl number, Sc is Schmidt number, Gr is thermal Grashof number, Gc is mass Grashof number, M is magnetic field, K is porosity, R is the radiation, Q is the heat source and Sr is the Soret.*

Numerical Solution

In this study, we adopted a uniform grid spacing in both x and y directions. We treated Δx and Δy as constant values, but noted that they do not have to be equal. The grid points are identified by two indices: i, which increases in the positive x-direction, and j, which increases in the positive y-direction. If point P is located at (i, j), the point to its right is (i+1, j), the point to its left is (i-1, j), the point above it is (i, j+1), and the point below it is (i, j-1). The finite difference method's fundamental principle is to approximate derivatives using the values of the function at these grid points.

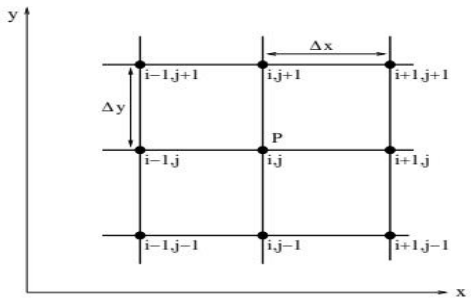

Figure 1: Implicit finite difference system grid

The equations (8), (9), and (10) are unsteady, coupled, nonlinear partial differential equations that need to be solved under the initial and boundary conditions specified in equation (11). However, obtaining exact or approximate solutions for these equations is challenging. Therefore, the implicit finite difference scheme was employed to solve them. The implicit finite difference scheme for the differential terms in the governing equations (8), (9), and (10) is determined as:

$$\frac{\partial u}{\partial t}=\frac{U_i^{j+1}-U_i^j}{\Delta t}, \frac{\partial u}{\partial y}=\frac{U_i^{j+1}-U_i^j}{\Delta y}, \frac{\partial^2 u}{\partial y^2}=\frac{\left(U_{i-1}^{j+1}-2U_i^{j+1}+U_{i+1}^{j+1}\right)}{\Delta y^2}, \frac{\partial\theta}{\partial t}=\frac{\theta_i^{j+1}-\theta_i^j}{\Delta t},$$
$$\frac{\partial\theta}{\partial y}=\frac{\theta_i^{j+1}-\theta_i^j}{\Delta y}, \frac{\partial^2\theta}{\partial y^2}=\frac{\left(\theta_{i-1}^{j+1}-2\theta_i^{j+1}+\theta_{i+1}^{j+1}\right)}{\Delta y^2}, \frac{\partial C}{\partial t}=\frac{C_i^{j+1}-C_i^j}{\Delta t}, \frac{\partial C}{\partial y}=\frac{C_i^{j+1}-C_i^j}{\Delta y},$$
$$\frac{\partial^2 C}{\partial C^2}=\frac{\left(C_{i-1}^{j+1}-2C_i^{j+1}+C_{i+1}^{j+1}\right)}{\Delta y^2}. \quad (12)$$

www.ijprems.com
editor@ijprems.com

INTERNATIONAL JOURNAL OF PROGRESSIVE RESEARCH IN ENGINEERING MANAGEMENT AND SCIENCE (IJPREMS)
(Int Peer Reviewed Journal)
Vol. 05, Issue 10, October 2025, pp : 569-579

e-ISSN : 2583-1062
Impact Factor : 7.001

Considering the implicit finite difference scheme of *equation (12) and substitute into* equations (8), (9) and (10) respectively.

$$\frac{U_i^{j+1}-U_i^j}{\Delta t} = \propto \frac{\left(U_{i-1}^{j+1}-2U_i^{j+1}+U_{i+1}^{j+1}\right)}{\Delta y^2} + (1-\propto)\frac{\left(U_{i-1}^{j}-2U_i^{j}+U_{i+1}^{j}\right)}{\Delta y^2} + Gr\theta_i^j + GmC_i^j - MU_i^j - K^{-1}U_i^j \quad (13)$$

The Implicit finite difference scheme of the equation (9), is solved as follows;

$$\frac{\theta_i^{j+1}-\theta_i^j}{\Delta t} = \frac{1}{Pr}\left[\propto \frac{\left(\theta_{i-1}^{j+1}-2\theta_i^{j+1}+\theta_{i+1}^{j+1}\right)}{\Delta y^2} + (1-\propto)\frac{\left(\theta_{i-1}^{j}-2\theta_i^{j}+\theta_{i+1}^{j}\right)}{\Delta y^2}\right] - \frac{1}{Pr}\left(R-Q\theta_i^j\right) \quad (14)$$

The Implicit finite difference scheme of the equation (10), is solved as follows;

$$\frac{C_i^{j+1}-C_i^j}{\Delta t} = \frac{1}{Sc}\left[\propto \frac{\left(C_{i-1}^{j+1}-2C_i^{j+1}+C_{i+1}^{j+1}\right)}{\Delta y^2} + (1-\propto)\frac{\left(C_{i-1}^{j}-2C_i^{j}+C_{i+1}^{j}\right)}{\Delta y^2}\right] - KC_i^j + Sr\left[\propto \frac{\left(\theta_{i-1}^{j+1}-2\theta_i^{j+1}+\theta_{i+1}^{j+1}\right)}{\Delta y^2} + (1-\propto)\frac{\left(\theta_{i-1}^{j}-2\theta_i^{j}+\theta_{i+1}^{j}\right)}{\Delta y^2}\right] \quad (15$$

We derived equations (16), (17), and (18) using the implicit scheme, which will be solved and visualized using MATLAB, with corresponding plots generated

$$.-r_1U_{i-1}^{j+1} + (1+2r)U_i^{j+1} - r_1U_{i+1}^{j+1} = r_2U_{i-1}^{j} + (1-2r_2-r_3-r_4)U_i^j + r_2U_{i+1}^j + \Delta tGr\theta_i^j + \Delta tGmC_i^j \quad (16)$$

$$-r_1\theta_{i-1}^{j+1} + (Pr+2r_1)\theta_i^{j+1} - r_1\theta_{i+1}^{j+1} = r_2\theta_{i-1}^{j} + (Pr-2r_2+r_5)\theta_i^j + \Delta tR + r_2\theta_{i+1}^j \quad (17)$$

$$-r_1C_{i-1}^{j+1} - r_7\theta_{i-1}^{j+1} + (Sc+2r_1)C_i^{j+1} + 2r_7\theta_i^{j+1} - r_1C_{i+1}^{j+1} - r_7\theta_{i+1}^{j+1} = r_2C_{i-1}^{j} + r_8\theta_{i-1}^{j} + (Sc-2r_2-r_6Sc)C_i^j - 2r_8\theta_i^j + r_2C_{i+1}^j + r_8\theta_{i+1}^j \quad (18)$$

Where $r_1 = \frac{\propto \Delta t}{\Delta y^2}$, $r_2 = \frac{(1-\propto)\Delta t}{\Delta y^2}$, $r_3 = \Delta tM$, $r_4 = \frac{\Delta t}{K}$, $r_5 = \Delta tQ$, $r_6 = \Delta tK$,

$$r_7 = \frac{\propto \Delta tScSr}{\Delta y^2}, and\ r_8 = \frac{(1-\propto)\Delta tScSr}{\Delta y^2}$$

The mesh size along y- direction and time t-direction are Δy and Δt respectively while the index i refers to space y and j refers to time t . The finite difference equations (16), (17) and (18)*at every internal nodal point on a particular n-level constitute a tridiagonal system of equations which are solved by using the Thomas algorithm.*

4. RESULTS AND DISCUSSION

This study investigated the capabilities of the MATLAB software package, focusing on its use in coding numerical solutions, creating visualizations, and analyzing the effects of various physical flow parameters. The parameters examined included the thermal Grashof number (Gr), Prandtl number (Pr), heat source (Q), Soret number (Sr), mass Grashof number (Gc), radiation (R), magnetic field (M), porosity (K), and Schmidt number (Sc). Unless otherwise stated, these parameters were held constant throughout the calculations. The specific values used in the study were: Prandtl number (Pr) = 0.70, Schmidt number (Sc) = 0.57, radiation (R) = 0.10, magnetic field (M) = 1, porosity (K) = 1, thermal Grashof number (Gr) = 5, mass Grashof number (Gc) = 5, heat source (Q) = 1. and t = 0.2.

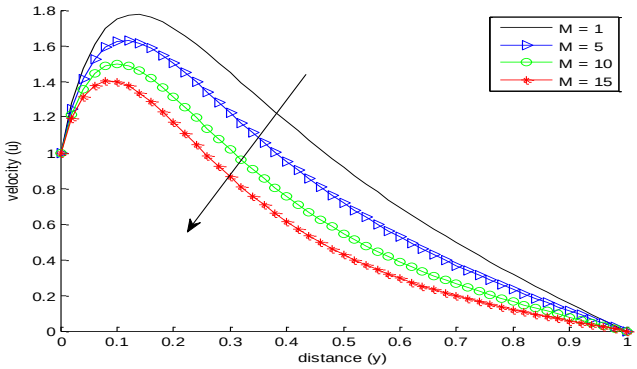

Figure 2 : *influence of magnetic parameter (M) on velocity profile when Pr = 0.70, dt = 0.004, dy = 1/m, y = 0:dy:1, dy2 = 2.0*dy, t = 0.2, K = 1, Gr = 5, Gc = 5, Sc = 0.57, and R = 0.10.*

www.ijprems.com
editor@ijprems.com

INTERNATIONAL JOURNAL OF PROGRESSIVE RESEARCH IN ENGINEERING MANAGEMENT AND SCIENCE (IJPREMS)
(Int Peer Reviewed Journal)
Vol. 05, Issue 10, October 2025, pp : 569-579

e-ISSN : 2583-1062
Impact Factor : 7.001

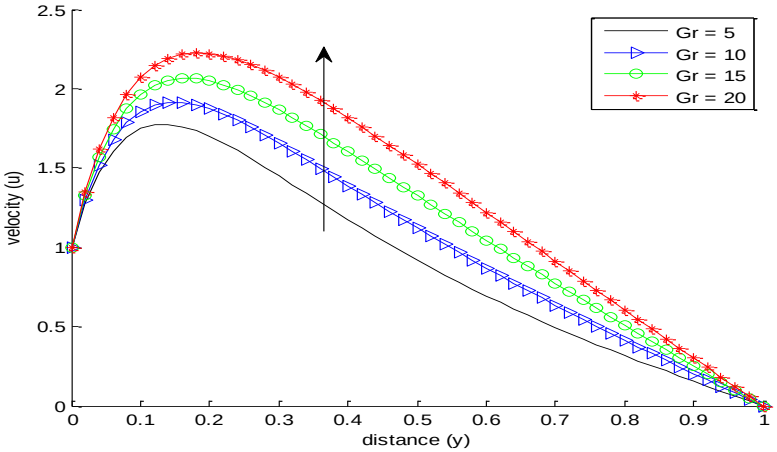

Figure 3: Effect of Grashof number (Gr) on velocity profile when Pr = 0.70, dt = 0.004, dy = 1/m, y = 0:dy:1, dy2 = 2.0*dy, t = 0.2, K = 1, Gc = 5, Sc = 0.57, R = 0.10 and M = 1

Figures 2 and 3 demonstrate the impact of the magnetic parameter (M = 1, 5, 10, 15) and thermal Grashof number (Gr = 5, 10, 15, 20) on velocity profiles. Figure 2 illustrates the effect of increasing magnetic fields, which results in a decrease in velocity due to the resistance exerted by the magnetic field on the fluid's motion. This is consistent with the findings of Usman and Sanusi (2023). Conversely, Figure 3 shows that an increase in the magnetic parameter, while keeping other parameters constant, leads to an increase in fluid velocity. This suggests that the magnetic field can interact with the fluid, causing it to accelerate.

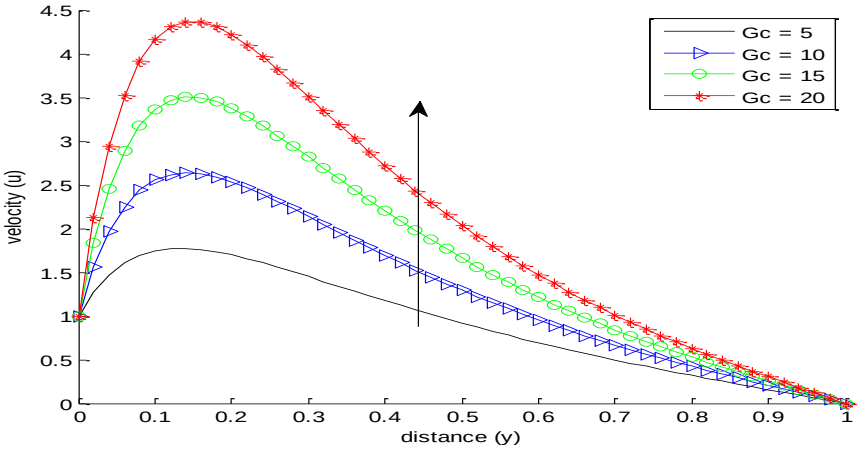

Figure 4: Effect of Mass Grashof number on velocity profile when Pr = 0.70, dt = 0.004, dy = 1/m, y = 0:dy:1, dy2 = 2.0*dy, t = 0.2, K = 1, Gr = 5, Sc = 0.57, R = 0.10, and M = 1

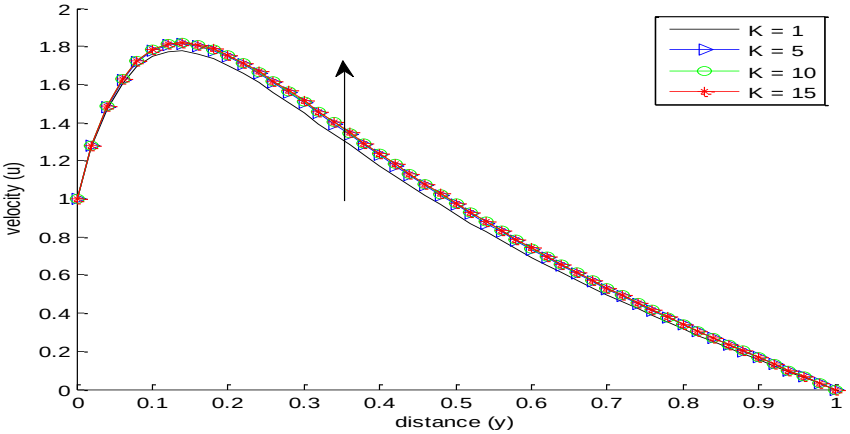

Figure 5: Effect of Porosity parameter (K) on velocity profile when Pr = 0.70, dt = 0.004, dy = 1/m, y = 0: dy: 1, dy2 = 2.0*dy, t = 0.2, K = 1, Gr = 5,Gc = 5,Sc = 0.57,R = 0.10, and M = 1

www.ijprems.com
editor@ijprems.com

INTERNATIONAL JOURNAL OF PROGRESSIVE RESEARCH IN ENGINEERING MANAGEMENT AND SCIENCE (IJPREMS)
(Int Peer Reviewed Journal)
Vol. 05, Issue 10, October 2025, pp : 569-579

e-ISSN : 2583-1062
Impact Factor : 7.001

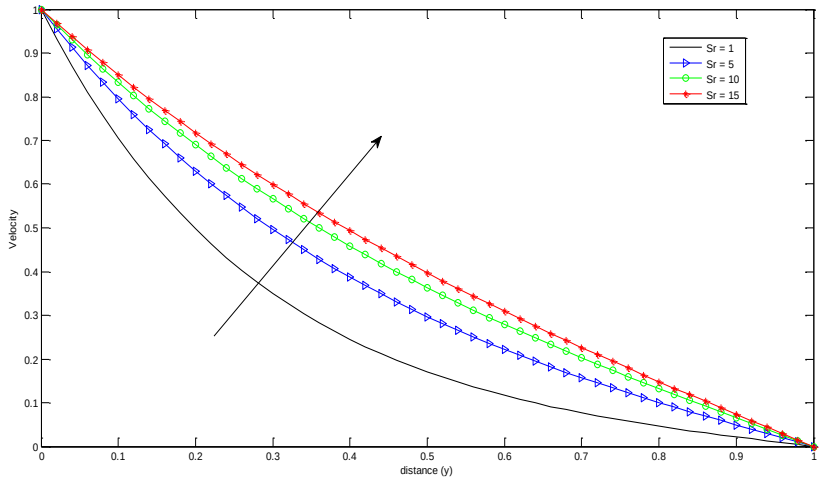

Figure 6: Effect of Soret number (Sr) on Velocity profile when M = 1, dt = 0.2, dy = 1/m, y = 0:dy:1, dy2 = 2.0*dy, Gr = 5, Gc = 5, R = 0.10, Kr = 1 and Sc = 0.57.

Figures 4, 5, and 6 illustrate the influence of the Mass Grashof number (Gr), the Permeability parameter (K), and time (t) on fluid velocity profiles. Figure 4 demonstrates how fluid velocity increases with increasing Mass Grashof number values, while keeping other parameters constant. Similarly, Figure 5 shows that fluid velocity increases significantly as Permeability parameter values increase, due to the reduced obstacles to fluid flow in more permeable media. This enables the fluid to pass through a porous material more efficiently and at higher speeds. Figure 6 further shows that, for fixed values of the other parameters, fluid velocity increases with time, indicating a gradual increase in fluid flow over time.

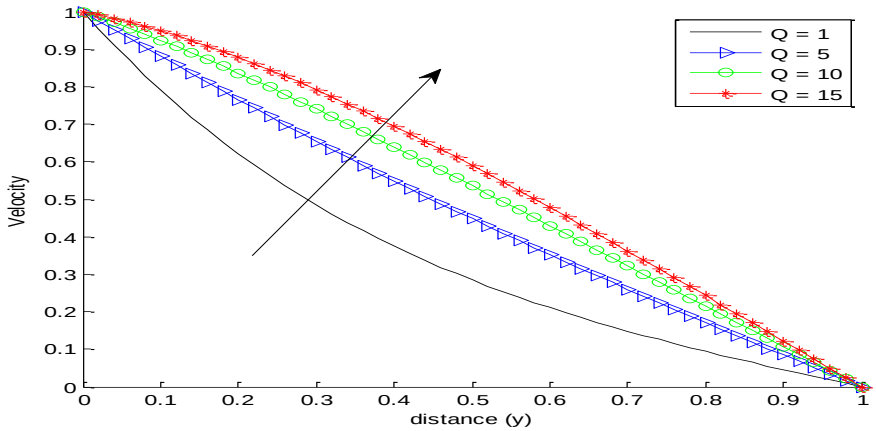

Figure 7: Effect of Heat source parameter on velocity profile when Pr = 0.70, dt = 0.004, dy = 1/m, y = 0:dy:1, dy2 = 2.0*dy, K = 1, Gr = 5, Gc = 5, Sc = 0.57, R = 0.10, and M = 1.

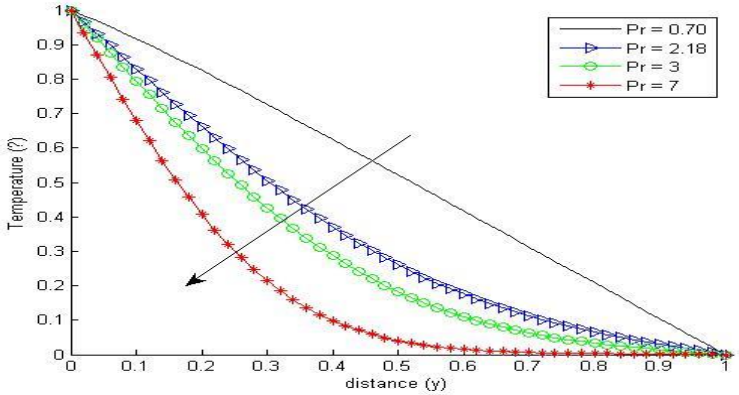

Figure 8: Effect of Prandtl number (Pr) on temperature profile when M = 1, dt = 0.004, dy = 1/m, y = 0:dy:1, dy2 = 2.0*dy, t = 0.2, Gr = 5, Gm = 5, Q = 1, R = 0.10, and Sc = 0.57.

www.ijprems.com
editor@ijprems.com

INTERNATIONAL JOURNAL OF PROGRESSIVE RESEARCH IN ENGINEERING MANAGEMENT AND SCIENCE (IJPREMS)
(Int Peer Reviewed Journal)
Vol. 05, Issue 10, October 2025, pp : 569-579

e-ISSN : 2583-1062
Impact Factor : 7.001

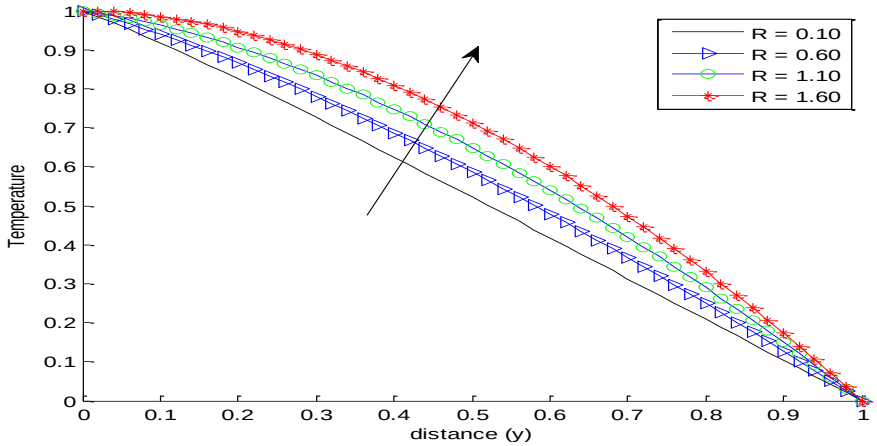

Figure 9: Effect of Radiation parameter (R) on temperature profile when M = 1, dt = 0.004, dy = 1/m, y = 0:dy:1, dy2 = 2.0*dy, Pr = 0.70 t = 0.2, Gr = 5, Gm = 5, Q = 1, and Sc = 0.57.

The impact of of heat source (Q = 1, 3, 7, 10), Prandtl number (Pr = 0.70, 2.18, 3.0, 7.0) and Radiation (R = 0.10, 0.60, 1.10, 1.60) parameters on the temperature profile are shown in Figure 7, 8, and 9. The graph in Figure 7 indicated that as the heat source parameter increases, the velocity of the fluid increases. The impact of changing the Prandtl number (Pr = 0.70, 2.18, 3.0, 7.0) on the temperature gradient is shown in Figure 8. The graph shows that when the Prandtl number increases, temperature decreases. This is physically true because a higher Prandtl number indicates that thermal diffusion is slower than momentum diffusion, leading to a thinner thermal boundary layer. Figure 9 depicts that the temperature increases with an increase in the radiation parameter, this is physically true because the temperature rises as the system absorbs more energy from radiation sources. The result establishes an excellent agreement with work of Sharma et al. (2022).

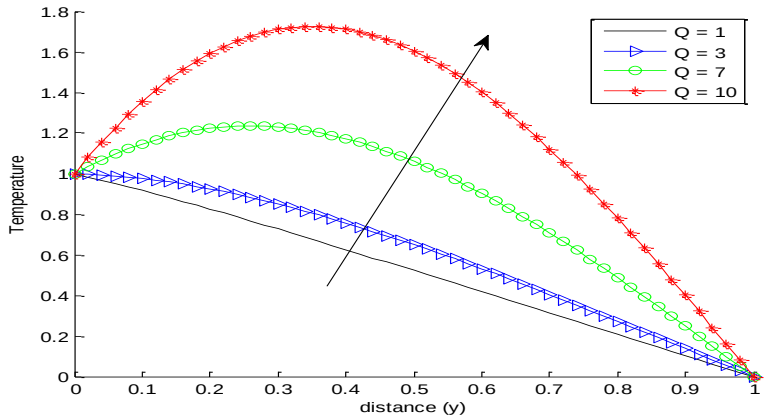

Figure 10: Effect of Heat source Parameter (Q) on temperature profile when M = 1, dt = 0.004, dy = 1/m, y = 0:dy:1, dy2 = 2.0*dy,t = 0.2, Gr = 5, Gm = 5, R = 0.10, and Sc = 0.57.

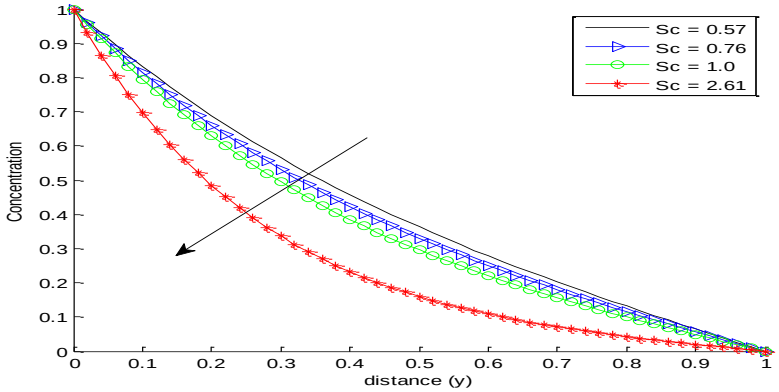

Figure 11: Effect of Schmidt number (Sc) on Concentration profile when M = 1, dt = 0.2, dy = 1/m, y = 0:dy:1, dy2 = 2.0*dy, Gr = 5, Gc = 5, R = 0.10, t = 0.2,Kr = 1 and Sc = 0.57.

www.ijprems.com
editor@ijprems.com

INTERNATIONAL JOURNAL OF PROGRESSIVE RESEARCH IN ENGINEERING MANAGEMENT AND SCIENCE (IJPREMS)
(Int Peer Reviewed Journal)
Vol. 05, Issue 10, October 2025, pp : 569-579

e-ISSN : 2583-1062
Impact Factor : 7.001

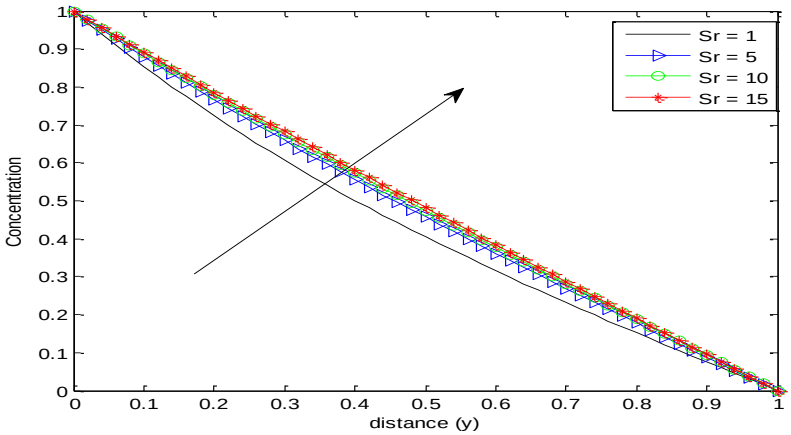

Figure 12: Effect of Soret number (Sr) on Concentration profile when M = 1, dt = 0.2, dy = 1/m, y = 0:dy:1, dy2 = 2.0*dy, Gr = 5, Gc = 5, R = 0.10, Kr = 1 and Sc = 0.57.

As shown in Figure 10, the temperature of the system increases as the heat source parameter increases. This is because the higher heat source parameter supplies more energy to the system, causing its temperature to rise due to increased thermal energy input. This finding is consistent with the results of Khan et al. (2022). Figure 11 demonstrates the impact of the Schmidt number (Sc) on concentration. Notably, as the Schmidt number increases, the concentration decreases. This is because a higher Schmidt number allows the fluid to transfer momentum more efficiently than mass, resulting in a decrease in concentration as less mass is transferred. In contrast to Figure 12, the concentration of the mixture increases as the Soret number (Sr) is increased, while keeping other parameters constant. This indicates that as the Soret number rises, thermal gradients have a more significant impact on the movement of species within the mixture compared to concentration gradients. The temperature gradient drives the species movement, resulting in increased concentrations in the hotter regions.

5. CONCLUSION

This research investigates the unsteady behavior of magneto-hydrodynamic (MHD) free convection flow over a vertically oscillating plate embedded in a porous medium. The study takes into account the effects of the Soret effect and a heat source on the flow. A numerical solution using an implicit finite difference method is employed to compute the velocity, temperature, and concentration fields that govern the flow. The study examines the impact of various parameters, including the magnetic field parameter, radiation parameter, Grashof number, mass Grashof number, Prandtl number, Schmidt number, porosity parameter, Soret number, and heat source parameter. The results show that the velocity decreases with increasing magnetic field parameter, and other key findings are presented through graphical representations. The key findings are as follows: First, the velocity decreases as the magnetic field parameter (M), Prandtl number (Pr), radiation parameter (R), permeability of the porous medium (K), and Schmidt number (Sc) increase. Second, an increase in the heat source parameter (Q) leads to an acceleration of the fluid velocity. Third, higher values of the Grashof number (Gr), mass Grashof number (Gm), and porous medium parameter (K) result in enhanced fluid velocity. Fourth, the temperature of the fluid decreases with increasing Prandtl number (Pr), while it rises with higher radiation (R) and heat source (Q) parameters. Fifth, the concentration diminishes as the Schmidt number (Sc) increases. Sixth, an increase in the Soret parameter leads to an enhancement in both the velocity and concentration of the fluid.

ACKNOWLEDGEMENT

This study was funded by the Tertiary Education Trust Fund (TETFund) through the 2025 Institutional Based Research (IBR) projects at Kebbi State Polytechnic Dakin-Gari, Kebbi State, Nigeria.

6. REFERENCES

[1] Akcay, S., Akdag, U. and Palancioglu, H., (2020). Experimental investigation of mixed convection on an oscillating vertical flat plate. International Communications in Heat and Mass Transfer, 113, 104528.

[2] Alwawi, F.A., Alkasasbeh, H.T., Rashad, A.M. and Idris, R., (2020). MHD natural convection of Sodium Alginate Casson nanofluid over a solid sphere. Results in physics, 16, p.102818.

[3] Amar, N., Kishan, N., Goud, B.S., (2022). MHD heat transfer flow over a moving wedge with convective boundary conditions with the influence of viscous dissipation and internal heat generation/absorption. Heat Transfer, 51(6), pp. 5015-5029.

[4] Bafakeeh O. T., Raza A., Khan U. S., Khan M. I., Nasr A., Khedher N.B. and Tag-Eldin E.M. (2022). Physical interpretation of Nanofluid (Copper Oxide and Silver) with slip and mixed convection effects: Application of fractional derivatives; Applied Sciences, 12 (21), 10.3390/app122110860.

[5] Bilal, S., Shah, I.A., Ghachem, K., Aydi, A. and Kolsi, L., (2023). Heat Transfer Enhancement of MHD Natural Convection in a Star-Shaped Enclosure, Using Heated Baffle and MWCNT–Water Nanofluid. Mathematics, 11(8), p.1849. https://doi.org/10.3390/ math11081849.

[6] Chitra M. and Suhasini M. (2018). Effect of unsteady oscillatory MHD flow through a porous medium in porous vertical channel with chemical reaction and concentration, National Conference on Mathematical Techniques and its Applications, 012039, doi :10.1088/1742-6596/1000/1/012039

[7] Elbashbeshy E. M. A., H. G. Asker, and B. Nagy, (2022). The effects of heat generation absorption on boundary layer flow of a nanofluid containing gyrotactic microorganisms over an inclined stretching cylinder, Ain Shams Engineering Journal, 13(5), pp. 101690 doi: 10.1016/j.asej.2022.101690.

[8] Fu, W.S. and Tong, B.H., (2017). Numerical investigation of heat transfer from a heated oscillating cylinder in a cross flow. International Journal of Heat and Mass Transfer, 45(14), pp.3033–3043.

[9] Hussain, S.M., Goud, B.S., Madheshwaran, P., Jamshed, W., Pasha, A.A., Safdar, R., Arshad, M., Ibrahim, R.W., Ahmad, M.K., (2022). Effectiveness of Nonuniform Heat Generation (Sink) and Thermal Characterization of a Carreau Fluid Flowing across a Nonlinear Elongating Cylinder: A Numerical Study. ACS Omega, 7(29), pp. 25309–25320.

[10] Jahangiri, M. and Delbari, O., (2020). Heat transfer correlation for two phase flow in a mixing tank. Journal of Heat and Mass Transfer research, 7(1), pp.1-10.

[11] Khalid, A., Khan, I. and Shafie, S., (2017). Free convection flow of micropolar fluids over an Oscillating vertical plate. Malaysian Journal of Fundamental Applied Science, 13(4), pp.654–658.

[12] Khan M., M. Yasir, A. Saleh, S. Sivasankaran, Y. Rajeh, and A. Ahmed, (2022). Variable heat source in stagnation-point unsteady flow of magnetized Oldroyd-B fluid with cubic autocatalysis chemical reaction, Ain Shams Engineering Journal, 13(3), pp. 101610 doi: 10.1016/j.asej.2021.10.005.

[13] Krishna, M.V., Reddy, M.G., Chamkha, A.J., (2019). Heat and mass transfer on MHD flow over an infinite non-conducting vertical flat porous plate. Journal of Porous Media, 46 (1), pp. 1-25.

[14] Muhammad, S. D., Aisha U. D., and Yale, I. D., (2024) A Study on Unsteady Magneto-Hydrodynamics (Mhd) Free Convective Flow Past A Vertical Oscillating Plate Through A Porous Medium In The Presence Of Heat Source, Dutse Journal of Pure and Applied Sciences, 10(2b), pp. 353-365.

[15] Muthucumaraswamy, R. and Ghetta E. (2013) Chemical Reaction Effects on MHD Flow Past a Linearly Accelerated Vertical Plate with Variable Temperature and Mass Diffusion in the Presence of Thermal Radiation, International Journal of Applied Mechanics and Engineering.vol.18, No.3, pp.727-737

[16] Nemati M., M. Sefid, and A. R. Rahmati, (2021). Analysis of the Effect of Periodic Magnetic Field, Heat Absorption / Generation and Aspect Ratio of the Enclosure on Non-Newtonian Natural Convection, Journal of Heat and Mass Transfer Research,8, pp. 187–203 doi: 10.22075/JHMTR.2021.22119.1322.

[17] Noor N. A. M., Shafie, S., and Admon, M. A. (2020). Unsteady MHD squeezing flow of Jeffrey fluid in a porous medium with thermal radiation, heat generation/absorption and chemical reaction. Physica Script, 95(10), 105213.

[18] Okuyade W.I.A., T.M. Abbey, A.T. Gima-Laabel, (2018). "Unsteady free convective chemically reacting fluid flow over a vertical plate with thermal radiation, Dufour, Soret and constant suction effects" Alex. Eng. J. 57, 3863– 3871,https://doi.org/10.1016/j.aej.2018.02.006.

[19] Pradhan, B., Das, S.S., Paul, A.K. and Dash, R.C., (2017). Unsteady free convection flow of a viscous incompressible polar fluid past a semi-infinite vertical porous moving plate. International Journal of Applied Engineering Research, 12(21), pp.10958–10963.

[20] Pourgholam, M., Izadpanah, E., Motamedi, R. and Habibi, S.E., (2015). Convective heat transfer enhancement in a parallel plate channel by means of rotating or oscillating blade in the angular direction. Applied Thermal Engineering, 78(5), pp.248–257.

[21] Rahman, A. and Tafti, D., (2020). Characterization of heat transfer enhancement for an oscillating flat plate-fin. International Journal of Heat and Mass Transfer, 147, 119001.

[22] Sahin Ahmed and Karabi Kalita (2014): "Unsteady MHD Chemically Reacting Fluid through a Porous medium bounded by a Non-Isothermal Impulsively-Started Vertical Plate: A Numerical Technique" Journal of Naval Architecture and Marine Engineering, Volume 11, pp. 29-54. http://dx.doi.org/10.3329/jname.v11i1.10269.

[23] Sarhan, A.R., Karim, M.R., Kadhim, Z.K. and Naser, J., (2019). Experimental investigation on the effect of vertical vibration on thermal performances of rectangular flat plate. Experimental Thermal and Fluid Science, 101, pp.231–240.

[24] Sharma T., Sharma P. and Kumar N. (2022). Study of dissipative MHD oscillatory unsteady free convective flow in a vertical channel occupied with the porous material in the presence of heat source effect and thermal radiation, International Symposium on Fluids and Thermal Engineering, 012012. doi:10.1088/1742-6596/2178/1/012012.

[25] Sheikholeslami M., (2022). Numerical investigation of solar system equipped with innovative turbulator and hybrid nanofluid, Solar Energy Materials and Solar Cells, 243, pp. 111786.

[26] Usman H. and Sanusi S. (2023). Heat and mass transfer analysis for the mhd flow of Casson nanofluid in the presence of thermal radiation, FUDMA Journal of Sciences 7(2), pp 188 – 198. https:doi.org/10.33003/fjs-2023-0702-1728

[27] Yasir M., A. Ahmed, M. Khan, Z. Iqbal, and M. Azam, (2022). Impact of ohmic heating on energy transport in double diffusive Oldroyd-B nanofluid flow induced by stretchable cylindrical surface, Proceedings of the Institution of Mechanical Engineers, Part E: Journal of Process Mechanical Engineering, 0(0) doi: 10.1177/09544089211064116.